# Factorization of products of discontinuous functions applied to Fourier–Bessel basis

**Evgeny Popov, Michel Nevière, and Nicolas Bonod**

*Institut Fresnel, Case 161, Unité Mixte de Recherche (UMR 6133), Faculté des Sciences et Techniques de St.-Jérôme, 13397 Marseille Cedex 20, France*

Received May 13, 2003; revised manuscript received August 1, 2003; accepted September 8, 2003

The factorization rules of Li [J. Opt. Soc. Am. A **13**, 1870 (1996)] are generalized to a cylindrical geometry requiring the use of a Bessel function basis. A theoretical study confirms the validity of the Laurent rule when a product of two continuous functions or of one continuous and one discontinuous function is factorized. The necessity of applying the so-called inverse rule in factorizing a continuous product of two discontinuous functions in a truncated basis is demonstrated theoretically and numerically. © 2004 Optical Society of America

*OCIS codes:* 000.3860, 050.1940, 000.4430, 070.2590.

## 1. INTRODUCTION

Numerical modeling of electromagnetic diffraction requires, in most instances, the factorization of products of discontinuous functions represented in a given basis. This is an intrinsic characteristic of the electromagnetic vectorial problem, which comes from the continuity of the normal component $D_N$ of the vector of electric induction $\mathbf{D} = \epsilon\mathbf{E}$, which implies a discontinuity of the normal component of the electric field vector $\mathbf{E}$ across physical interfaces characterized by a jump of electric permittivity $\epsilon$. The classical Laurent rule,[1] representing the product $\epsilon\mathbf{E}$ as a convolution-type sum, is valid when one is considering an infinite (and thus complete) set of basic functions. However, numerical modeling requires truncation of the basis, owing to obvious memory and computing time limitations. When one is studying periodic structures (having one-, two-, or three-dimensional periodicity), the natural basis consists of exponential functions involving the corresponding Cartesian coordinates. Cylindrical geometry requires a Fourier–Bessel basis because of the obvious periodicity with respect to a $2\pi$ rotation about the $z$ axis. The aim of this paper is to analyze theoretically and numerically the factorization rules when applied in Bessel function basis. The study could be useful in application of the differential method or rigorous-coupled-wave analysis, which are well-developed for gratings, to cylindrical or elliptical geometries. If the electric vector direction is parallel to the cylinder axis, all the field components are continuous functions of the radial coordinate, so that the Laurent rule suffices.[2] However, any other case of polarization and, in particular, the fiber-propagation problem, involves nonaxial electric field components, which are discontinuous across the fiber surface, and thus require special analysis of the factorization rules.[1,3]

## 2. FACTORIZATION RULES

Let us consider three functions $f$, $g$, and $h$ of a given variable $x$, the third function being the product of the first two:

$$h(x) = g(x)f(x). \tag{1}$$

We consider a set of basic continuous functions $\{\varphi_m(x)\}$ chosen to form a complete basis so that the functions $f$ and $h$ can be represented as a linear combination of the basic functions:

$$f(x) = \sum_{m=1}^{\infty} f_m \varphi_m(x). \tag{2}$$

The subscript $m$ could be a discrete or a continuous variable, depending on the basis. When $m$ is continuous, the sum over $m$ in Eq. (2) is replaced by an integral.

Numerical treatment requires truncation of the sum to a limited number of terms, say, $M$, which introduces some approximation to $f(x)$. Its approximate value will be

$$f^{(M)}(x) = \sum_{m=1}^{M} f_m \varphi_m(x). \tag{3}$$

The $m$th component of $f(x)$ represents the projection of $f$ on the $m$th basic function,

$$f_m = \langle f(x) | \varphi_m(x) \rangle, \tag{4}$$

where $\langle \ | \ \rangle$ represents the scalar product in the space of the considered functions. We assume orthonormality of the basis:

$$\langle \varphi_n(x) | \varphi_m(x) \rangle = \delta_{nm}. \tag{5}$$

In addition to the continuity of the basis functions, we assume the linearity of the scalar product in Eq. (4):

1084-7529/2004/010046-07$15.00 

$$\langle af(x) + bg(x)|\,\varphi_m(x)\rangle = a\langle f(x)|\,\varphi_m(x)\rangle + b\langle g(x)|\,\varphi_m(x)\rangle. \quad (6)$$

As an example, in the space of pseudoperiodic functions with period $d$, such that

$$f(x + d) = f(x)\exp(i\alpha_0 d), \quad (7)$$

the basis is discrete and is given by

$$\varphi_m(x) = \exp(i\alpha_m x) \equiv \exp\left[i\left(\alpha_0 + m\frac{2\pi}{d}\right)x\right], \quad (8)$$

and the scalar product is defined as an integral over the period:

$$\langle f|\,\varphi_m\rangle = \frac{1}{d}\int_0^d f(x)\bar{\varphi}_m(x)\mathrm{d}x, \quad (9)$$

where the overbar stands for complex conjugation.

A great variety of numerical studies in science require an answer to the following question: How can we better express the components of a product $h$ of two functions $f$ and $g$ as a function of their components in the basis truncated to $M$ basic functions?

We shall denote these components of $h$ as $h_m^{(M)}$. Here "better" is used in the sense of more rapidly converging with respect to $M$, i.e., minimizing the error introduced by truncation in Eq. (3) in comparison with Eq. (2), both equations applied to the function $h(x)$. One of the common tools for such a factorization consists of representing the components $h_m$ of the product as a sum (or integral) of products of the components of the two functions,

$$h_m = \sum_p g_{mp} f_p, \quad (10)$$

where

$$g_{mp} = \langle g(x)\varphi_p(x)|\,\varphi_m(x)\rangle. \quad (11)$$

In an exponential basis, Eq. (8), the sum in Eq. (10) is a convolution-type sum, called the Laurent rule, with $g_{nm}$ the elements of a Toeplitz matrix formed by the Fourier components of $g$:

$$g_{mp} = \frac{1}{d}\int_0^d g(x)\exp\left[i(p - m)\frac{2\pi}{d}x\right]. \quad (12)$$

The proof of the Laurent rule is straightforward from the given definitions and the linearity of Eq. (4):

$$\begin{aligned} h_m &= \langle g(x)f(x)|\,\varphi_m(x)\rangle \\ &= \left\langle g(x)\sum_{p=1}^{\infty} f_p\varphi_p(x)\,\middle|\,\varphi_m(x)\right\rangle \\ &= \sum_{p=1}^{\infty} f_p\langle g(x)\varphi_p(x)|\,\varphi_m(x)\rangle = \sum_{p=1}^{\infty} g_{mp}f_p. \end{aligned} \quad (13)$$

In 1996 Li[1] found that the Laurent rule is questionable when used in a truncated space of basic functions and that its validity (in the sense of better or worse convergence) depends on the continuity of the functions on which it is applied. More specifically, Li established three rules of factorization in the truncated Fourier space:

1. If the functions $f(x)$ and $g(x)$ have no concurrent jumps, i.e., if $f(x)$ is continuous at the points of discontinuity of $g(x)$ and vice versa, the Laurent rule, Eqs. (10) and (11), can be applied in the truncated basis. Thus we have

$$h_m^{(M)} = \sum_{p=1}^{M} g_{mp}f_p, \qquad m,p = 1{:}M, \quad (14)$$

and the components $g_{mp}$ are given by Eq. (11) for $m$, $p = 1{:}M$. Equation (14) will be called the *direct* rule.

2. If $f(x)$ and $g(x)$ are discontinuous at the same points but their product $h(x)$ is continuous at these points, it is better (more rapidly convergent) to apply the so-called *inverse* rule, replacing Eqs. (14) and (11) by the following expressions:

$$h_m^{(M)} = \sum_{p=1}^{M} (g_{\mathrm{inv}}^{(M)})_{mp}^{-1} f_p, \quad (15)$$

where $(-1)$ stands for matrix inversion and $g_{\mathrm{inv}}^{(M)}$ is an $M \times M$ matrix with the elements

$$g_{\mathrm{inv},mp} = \left\langle \frac{1}{g(x)}\varphi_p(x)\,\middle|\,\varphi_m(x)\right\rangle, \qquad m,p = 1{:}M. \quad (16)$$

The inverse rule thus requires the existence of $1/g(x)$ and the possibility of inverting the matrix $g_{\mathrm{inv}}^{(M)}$.

3. In any other case [simultaneous discontinuity of $f(x)$, $g(x)$, and $h(x)$], neither the direct nor the inverse rule gives a satisfactory convergence with respect to $M$.

Li established these rules for a truncated Fourier basis, explaining the empirical results obtained independently by Lalanne and Morris[4] and Granet and Guizal.[5] It is straightforward to demonstrate the validity of the direct and the inverse rules for any truncated basis of continuous functions, assuming the validity of a single hypothesis: Provided a complete basis consisting of an ordered infinite number of continuous functions and a given function $f(x)$, if a truncated set containing a finite number $M$ of these functions is considered, the convergence of the approximate value $f^{(M)}(x)$ given in Eq. (3) converges to $f(x)$ when $M$ tends to infinity. The hypothesis states that the convergence is more rapid [i.e., the error $\int \mathrm{d}x|f(x) - f^{(M)}(x)|^2$ is smaller for a given $M$] when $f(x)$ is a continuous function than when $f(x)$ is a discontinuous function. Stated briefly, this means the following: Continuous functions are better represented than discontinuous functions in a basis formed by continuous functions.

Here again, "better" means more rapidly converging with respect to the number of components. The validity of this hypothesis is almost self-evident, taking into account that a discontinuous function includes Dirac distributions in its derivative, which cannot be represented by a finite number of continuous functions[6] and that its reconstruction from its Fourier series gives rise to the Gibbs phenomenon. The demonstration of this property re-

mains beyond the scope of this paper. Of more immediate interest are its consequences.

Let us first assume that $f(x)$ is a continuous function and $g(x)$ is a discontinuous function of $x$. Then $h(x)$ is also a discontinuous function. The hypothesis ensures the relatively rapid convergence of Eq. (3), the rapidity depending on the form of $f(x)$. We can then rewrite Eq. (13) in the truncated space, using $M$ basic functions:

$$\begin{aligned} h_m^{(M)} &= \langle g(x) f^{(M)}(x) | \varphi_m(x) \rangle \\ &= \left\langle g(x) \sum_{p=1}^{M} f_p \varphi_p(x) \middle| \varphi_m(x) \right\rangle \\ &= \sum_{p=1}^{M} f_p \langle g(x) \varphi_p(x) | \varphi_m(x) \rangle \\ &= \sum_{p=1}^{M} g_{mp} f_p, \qquad 1 \leqslant m \leqslant M. \end{aligned} \tag{13'}$$

Equation (13′) represent the direct rule, as expressed in Eqs. (14) and (11) in the truncated basis of $M$ basic functions, whatever they are, not limited to exponentials of the form presented in Eq. (8). The only assumption is the convergence of Eq. (3), i.e., the validity of the hypothesis.

Second, let us consider the case where both $f(x)$ and $g(x)$ are discontinuous but their product $h(x)$ is a continuous function. This is a common situation, for example, in electromagnetism, where the normal component $D_N$ of the electric induction vector is continuous across any physical interface separating two media with different electrical permittivity. In case of isotropic permittivity, $D_N = \epsilon E_N$ and both $\epsilon$ and $E_N$ are discontinuous. Now we can apply the hypothesis to $h(x)$, which is continuous. If $1/g(x)$ exists, we can apply the direct rule to the product $f(x) = h(x)/g(x)$ by using Eq. (13) written in the truncated basis:

$$\begin{aligned} f_m^{(M)} &= \langle h(x)/g(x) | \varphi_m(x) \rangle = \left\langle \frac{1}{g(x)} \sum_{p=1}^{M} h_p \varphi_p(x) \middle| \varphi_m(x) \right\rangle \\ &= \sum_{p=1}^{M} h_p \left\langle \frac{1}{g(x)} \varphi_p(x) \middle| \varphi_m(x) \right\rangle = \sum_{p=1}^{M} g_{\mathrm{inv},mp} h_p. \end{aligned} \tag{17}$$

Now, it is sufficient to notice that by inverting the matrix $g_{\mathrm{inv}}^{(M)}$, Eq. (17) can be solved with respect to $h_p$ to obtain the inverse rule, Eqs. (15) and (16).

It must be pointed out that for an infinite basis, the two rules give identical results, but numerical applications cannot use infinite basis.

## 3. APPLICATION TO BESSEL FUNCTION BASIS

The basis based on Bessel functions is naturally used in cylindrical geometry, for example, in the modeling of optical fibers or in diffraction by a single hole or circular gratings. Owing to the periodicity with respect to the azimuthal angle $\theta$, any function $f$ of $r$, $\theta$, and $z$ can be expressed in a Fourier-series representation with respect to $\theta$:

$$f(r, \theta, z) = \sum_{n=-\infty}^{+\infty} f_n(r, z) \exp(in\theta). \tag{18}$$

The orthogonality of $\exp(in\theta)$ ensures the independence of the components that have a different subscript $n$. With the Hankel transform, the functions $f_n(r, z)$ can be developed in a Bessel function basis:

$$f_n(r, z) = \int_0^{\infty} k \mathrm{d}k \tilde{f}_n(k, z) J_n(kr). \tag{19}$$

Here $k$ could be considered, for example, as the $r$ component of the wave vector. By substituting Eq. (19) into Eq. (18), we obtain a Fourier–Bessel representation for $f$:

$$f(r, \theta, z) = \int_0^{\infty} k \mathrm{d}k \sum_{n=-\infty}^{+\infty} \tilde{f}_n(k, z) J_n(kr) \exp(in\theta). \tag{20}$$

In order to use the notation of the preceding section, we must change Eq. (18) slightly by including $k$ in the component $\tilde{f}_n$,

$$\hat{f}_n(k, z) = k \tilde{f}_n(k, z), \tag{21}$$

so that

$$f(r, \theta, z) = \int_0^{\infty} \mathrm{d}k \sum_{n=-\infty}^{+\infty} \hat{f}_n(k, z) J_n(kr) \exp(in\theta). \tag{22}$$

In what follows, the $z$ dependence will be omitted.

The orthogonality relations between the Bessel functions can be represented in the form

$$\int_0^{\infty} r \mathrm{d}r J_n(kr) J_n(k'r) = \frac{\delta(k - k')}{k}, \tag{23}$$

where $\delta$ is the Dirac delta function. The projection $\tilde{f}_n(k)$ of $f_n(r)$ over $J_n(kr)$ is given by the integral

$$\tilde{f}_n(k) = \int_0^{\infty} r \mathrm{d}r f_n(r) J_n(kr), \tag{24}$$

so that

$$\hat{f}_n(k) = k \tilde{f}_n(k) = k \int_0^{\infty} r \mathrm{d}r f_n(r) J_n(kr). \tag{25}$$

From Eqs. (19), (21), and (25) it is easy to derive the scalar product in the Bessel function space:

$$\langle f_n(r) | J_n(kr) \rangle = k \int_0^{\infty} r \mathrm{d}r f_n(r) J_n(kr). \tag{26}$$

Numerical applications usually require discretization, so the continuous variable $k$ has to be replaced by a discrete set of values $k_m = (m - 1)\Delta_k$, with $\Delta_k$ the distance between two consecutive values $k_m$ of $k$. The integral in Eq. (19) is replaced by a sum on $m$, and Eq. (19) takes the form of Eq. (2):

$$\begin{aligned} f_n(r) &= \int_0^{\infty} k \mathrm{d}k \tilde{f}_n(k, z) J_n(kr) \rightarrow \\ f_n(r) &= \sum_{m=1}^{\infty} k_m \Delta_k \tilde{f}_{n,m} J_n(k_m r) \\ &= \sum_{m=1}^{\infty} f_{n,m} J_n(k_m r), \end{aligned} \tag{27}$$

where, following Eq. (24),

$$\tilde{f}_{n,m} = \int_0^\infty r\mathrm{d}r f_n(r) J_n(k_m r),$$

$$f_{n,m} = \Delta_k k_m \tilde{f}_{n,m}. \tag{28}$$

The expression for $g_{mp}$ comes from Eqs. (11), (26), and (28):

$$g_{n,mp} = \Delta_k k_m \int_0^\infty r g_n(r) J_n(k_p r) J_n(k_m r)\mathrm{d}r. \tag{29}$$

## 4. NUMERICAL EXAMPLES

We now apply the direct and the inverse rules to several different functions in the following examples to illustrate the validity of the rules for different cases of discontinuous functions.

### A. Example 1

In this example, the function $g$ is defined as a piecewise constant,

$$g(r) = \begin{cases} 1, & r > R \\ Q, & r < R, \end{cases} \tag{30}$$

whereas the function $h_n$ is continuous and equal to the corresponding Bessel function:

$$h_n(r) = J_n(k_p r). \tag{31}$$

This choice permits analytical determination of the components:

$$h_{n,m} \equiv \Delta_k k_m \int_0^\infty h_n(r) J_n(k_m r) r\mathrm{d}r$$

$$= k_m \frac{\delta(k_m - k_p)}{k_m} \Delta_k \xrightarrow[\Delta_k \to 0]{} \delta_{mp}. \tag{32}$$

The last limit is due to the discretization and can be understood when one considers the application of the Dirac delta function to an arbitrary function $F$:

$$\int \delta(k_m - k_p) F(k_m)\mathrm{d}k_m = F(k_p) \xrightarrow{\text{discretization}}$$

$$\sum_m \delta_{mp} F_m = F_p, \qquad F(k_p) \to F_p.$$

Similar considerations apply for $g$:

$$g_{n,mq} \equiv \Delta_k k_m \int_0^\infty g_n(r) J_n(k_q r) J_n(k_m r) r\mathrm{d}r$$

$$= \Delta_k k_m \int_0^\infty J_n(k_q r) J_n(k_m r) r\mathrm{d}r$$

$$+ (Q - 1)\Delta_k k_m \int_0^R J_n(k_q r) J_n(k_m r) r\mathrm{d}r$$

$$= \delta_{mq} + (Q - 1) I_{n,mq}, \tag{33}$$

where

$$I_{n,mq} = \Delta_k k_m \int_0^R J_n(k_q r) J_n(k_m r) r\mathrm{d}r$$

and

$$g_{\mathrm{inv},n,mq} \equiv \Delta_k k_m \int_0^\infty \frac{1}{g_n(r)} J_n(k_q r) J_n(k_m r) r\mathrm{d}r$$

$$= \Delta_k k_m \int_0^\infty J_n(k_q r) J_n(k_m r) r\mathrm{d}r$$

$$+ \left(\frac{1}{Q} - 1\right) \Delta_k k_m \int_0^R J_n(k_q r) J_n(k_m r) r\mathrm{d}r$$

$$= \delta_{mq} + \left(\frac{1}{Q} - 1\right) I_{n,mq}. \tag{34}$$

We define a function $f_n(r) = 1/g(r) h_n(r)$ such that its Bessel components are equal to

$$f_{n,m} = \frac{1}{Q} \int_0^R J_n(k_m r) J_n(k_p r) r\mathrm{d}r \Delta_k k_m$$

$$+ \int_R^\infty J_n(k_m r) J_n(k_p r) r\mathrm{d}r \Delta_k k_m$$

$$= \delta_{mp} + \left(\frac{1}{Q} - 1\right) I_{n,mp} \equiv g_{\mathrm{inv},n,mp}. \tag{35}$$

Having established the analytical expression for all the components of the three functions, we can now compare the direct and the inverse rules when they are applied to the continuous product $h_n(r)$ of the two discontinuous functions $g$ and $f_n$. However, before that, it is worth noting that the expression for $f_{n,m}$ can be obtained from Eqs. (32) and (34) by use of the direct rule, independently of the truncation, provided that $M \geqslant k_p/\Delta_k$.

The direct rule for $h_{n,m}^{(M)}$ is written as

$$h_{n,m}^{(M,\mathrm{direct})} = \sum_{q=1}^{M} g_{n,mq}^{(M)} f_{n,q}^{(M)}$$

$$= \delta_{mp} + (Q - 1)\left(1 - \frac{1}{Q}\right)$$

$$\times \left(I_{n,mp} - \sum_{q=1}^{M} I_{n,mq} I_{n,qp}\right), \tag{36}$$

taking into account Eqs. (33) and (35).

The term in the last parentheses of Eq. (36) tends to zero as $M$ grows to infinity, owing to the second set of orthogonality relations for the Bessel functions:

$$r \int_0^\infty k\mathrm{d}k J_n(k r_1) J_n(k r_2) = \delta(r_1 - r_2), \tag{37}$$

so that

$$\sum_{q=1}^{M} I_{n,mq} I_{n,qp} \to \Delta_k k_m \int_0^\infty k_q \mathrm{d}k_q \int_0^R r_1 \mathrm{d}r_1 J_n(k_m r_1) J_n(k_q r_1) \times \int_0^R r_2 \mathrm{d}r_2 J_n(k_q r_2) J_n(k_p r_2)$$

$$= \Delta_k k_m \int_0^R r_1 \mathrm{d}r_1 J_n(k_m r_1) \int_0^R r_2 \mathrm{d}r_2 J_n(k_p r_2) \times \frac{\delta(r_1 - r_2)}{r_2}$$

$$= \Delta_k k_m \int_0^R r_1 \mathrm{d}r_1 J_n(k_m r_1) J_n(k_p r_1)$$

$$= I_{n,mp}. \tag{38}$$

Thus the direct rule, Eq. (36), gives the correct values, Eq. (32), for $h_{n,m} = \delta_{mp}$, only in the limit $M \to \infty$. However, when $M$ is finite, this relation is not rigorously fulfilled, and thus

$$h_{n,m}^{(M,\mathrm{direct})} \neq \delta_{mp} = h_{n,m}. \tag{39}$$

The inverse rule is written as

$$h_{n,m}^{(M,\mathrm{inv})} = \sum_{q=1}^{M} [g_{\mathrm{inv},n}^{(M)}]_{mq}^{-1} f_{n,q}^{(M)} \overset{\text{Eq. (35)}}{=} \sum_{q=1}^{M} [g_{\mathrm{inv},n}^{(M)}]_{mq}^{-1} g_{\mathrm{inv},n,qp}^{(M)} = \delta_{mp} \equiv h_{n,m}, \tag{40}$$

by using the definition of matrix inversion; i.e., the inverse rule gives the exact values of $h_{n,m}$ independently of the truncation parameter $M$. Of course, there is always some numerical error, owing to the matrix inversion.

Figure 1 presents the dependence of $h_{n,p}^{(M)}$, calculated numerically by using the direct and the inverse rules for different number $n$ of the Bessel functions. In all the examples, we take $R = 1$ and $Q = 10$. The value of $\Delta_k = 0.1$ is kept constant and low enough that its further reduction does not significantly influence the results. For a constant $\Delta_k$, the increase of $M$ results in increasing the maximum value of $k_m$, denoted on the abscissa axis as $k_{\mathrm{Max}} = M\Delta_k$. The value of $k_p$ in Eq. (31) is taken equal to 1.

As can be observed, the inverse rule always gives the correct value of 1 for $h_{n,p}^{(M)}$, whereas the direct rule gives results that converge more slowly toward the correct result. Moreover, the convergence is slower for the Bessel functions that have lower number $n$.

### B. Example 2

Let us consider a more complicated case, in some sense the opposite of example 1. Here the function $h_n$ has an infinite number of Bessel function components. We again take discontinuous functions $f_n$ and $g_n$ that have a continuous product $h_n$. The function $g_n(r)$ is the same as in the previous example, Eq. (30), whereas $h_n$ is chosen to have components independent of $m$:

$$h_n(r) = \frac{1}{r},$$

$$f_n(r) = \frac{1}{g_n(r)} h_n(r). \tag{41}$$

This choice gives constant values for all $h_{n,m}$, equal to $\Delta_k$, whatever $n$ and $m$ are, owing to the fact that

$$h_{n,m} \equiv \Delta_k k_m \int_0^\infty \frac{1}{r} J_n(k_m r) r \mathrm{d}r = \Delta_k k_m \frac{1}{k_m} = \Delta_k. \tag{42}$$

Figure 2 presents the values of $h_{1,1}^{(M)}/\Delta_k$ and $h_{1,5}^{(M)}/\Delta_k$ as a function of $k_{\mathrm{Max}} = M\Delta_k$ for $\Delta_k = 0.1$, $R = 1$, and $Q$

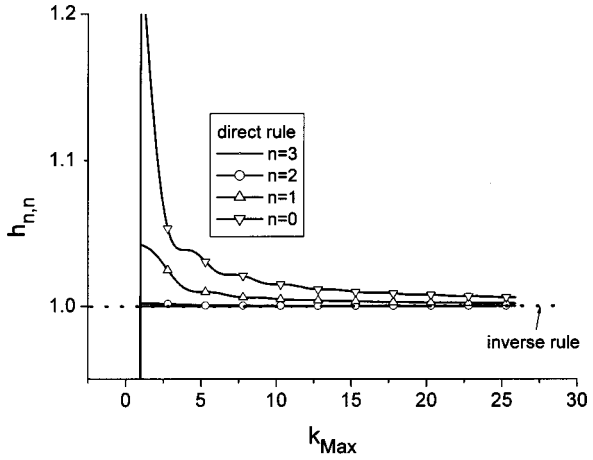


Fig. 1. Example 1. Convergence with respect to $k_{\mathrm{Max}} = 0.1M$ of the coefficient $h_{n,n}$ of the function $h_n(r) = J_n(r)$, calculated with the direct and the inverse rules for several values of $n$, shown in the insert.

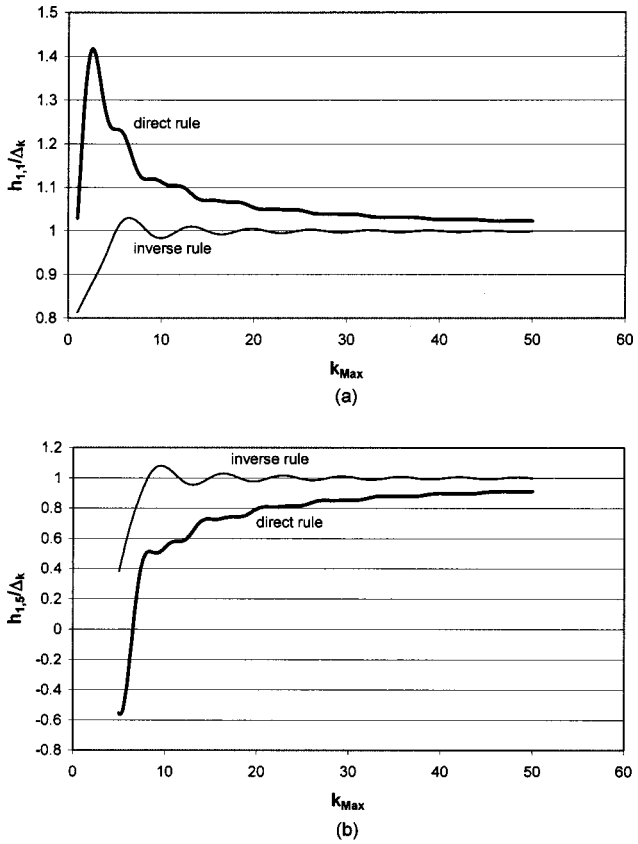


Fig. 2. Example 2. Convergence with respect to $k_{\mathrm{Max}} = 0.1M$ of the coefficients (a) $h_{1,1}$ and (b) $h_{1,5}$ of the function $h_n(r) = 1/r$.

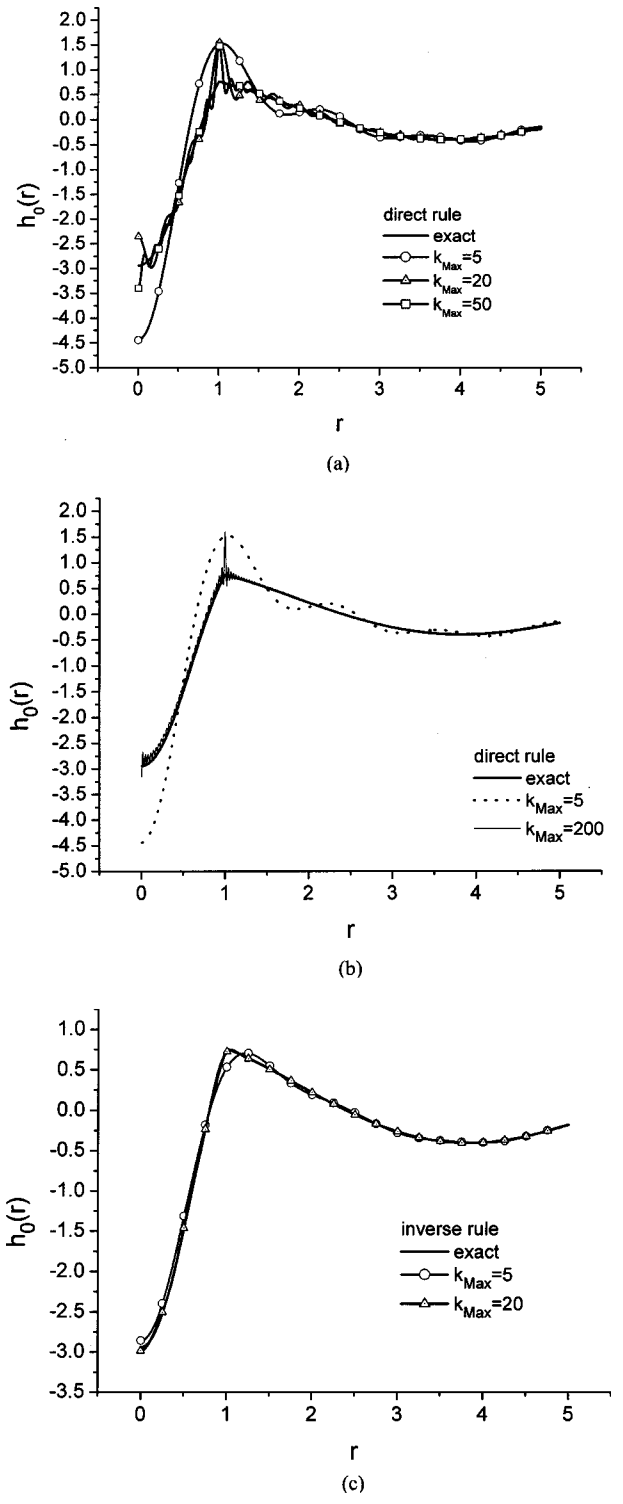


Fig. 3. Example 3. (a) Reconstruction of $h_0(r)$ with the direct rule with three different values of $k_{\mathrm{Max}}$, together with the exact plot, Eq. (46). (b) The same as in (a) but with $k_{\mathrm{Max}} = 200$. Gibbs phenomena are still observed. (c) The same as in (a) but with the inverse rule. The exact values cannot be distinguished from the curve obtained with $k_{\mathrm{Max}} = 20$. Gibbs phenomena are completely absent.

$= 10$. As can be observed, even in these difficult conditions (with $h_{n,m}/\Delta_k \equiv 1, \forall n, m$) the inverse rule ensures much better convergence than the direct rule.

### C. Example 3

The final example presents a more realistic situation, which is found in the modeling of optical fibers. Let us consider a dielectric cylinder with radius $R$ and refractive index $\nu_{(1)r<R} = \sqrt{Q}$. The surrounding medium has index $\nu_{(2)r>R} = 1$. In that case, a solution for the electromagnetic field that propagates along the $z$ axis with a constant of propagation $k_z$ can be sought in the form

$$f_n(r) \sim J_n(k_{r(1)}r), \qquad r < R,$$
$$f_n(r) \sim J_n(k_{r(2)}r), \qquad r > R, \tag{43}$$

with $k_{r(1)}$ and $k_{r(2)}$ being the radial components of the wave vector, determined from

$$k_{r(1)}^2 = k_0^2\nu_{(1)}^2 - k_z^2,$$
$$k_{r(2)}^2 = k_0^2\nu_{(2)}^2 - k_z^2, \tag{44}$$

where $k_0$ is the vacuum wave number.

If $f_n$ represents the $n$th component of the radial electric field, it is a discontinuous function of $r$ on the surface $r = R$, but its product with $g_n(r) = \nu^2$ [which also satisfies Eq. (30)] must be continuous. Let us keep the definition of $g_n$ given by Eq. (30). The choice of $f_n$ is made to have the same form as that given by Eq. (43),

$$f_n(r) = J_n(k_p r), \qquad r > R,$$
$$f_n(r) = \frac{1}{Q}\frac{J_n(k_pR)}{J_n(k_sR)}J_n(k_s r), \qquad r < R, \tag{45}$$

in such a way as to ensure that $h_n(r) = g_n(r)f_n(r)$ is a continuous product of discontinuous functions:

$$h_n(r) = J_n(k_p r), \qquad r > R,$$
$$h_n(r) = \frac{J_n(k_pR)}{J_n(k_sR)}J_n(k_s r), \qquad r < R. \tag{46}$$

As in the previous two examples, it is possible to determine analytically the Bessel components of $h_n$, $g_n$, and $f_n$, which are equal to

$$g_{n,mq} = \delta_{mq} + (Q - 1)I_{n,mq},$$
$$f_{n,m} = \delta_{mp} - \frac{1}{Q}I_{n,mp} + \frac{J_n(k_pR)}{J_n(k_sR)}I_{n,ms},$$
$$h_{n,m} = \delta_{mp} - I_{n,mp} + \frac{J_n(k_pR)}{J_n(k_sR)}I_{n,ms}. \tag{47}$$

On the other hand, we can calculate the components $h_{n,m}^{(M)}$ numerically, using the direct rule or the inverse rule, and compare their convergence when $M$ increases, with the exact values taken from Eq. (47). To better visualize the difference between the direct rule and the inverse rule, in this example we prefer to present not the convergence of $h_{n,m}^{(M)}$ but the reconstructed function,

$$h_n^{(M)}(r) = \sum_{m=1}^{M} h_{n,m}^{(M)}J_n(k_m r). \tag{48}$$

Figure 3 presents the $r$ dependence of $h_0(r)$ as given by Eq. (46) with $Q = 10$, $k_p = 1$, $k_s = 3$, $R = 1$, $n = 0$, and $\Delta_k = 0.1$. The values obtained by using Eq. (46) are

called exact values and are compared with the values calculated through Eq. (48) with the direct [Figs. 3(a) and 3(b)], and the inverse [Fig. 3(c)] rules. The direct rule leads to oscillations in the form of the Gibbs phenomenon, whose frequency increases as $M\,(k_{\mathrm{Max}} \equiv k_M = M\Delta_k)$. However, as is well known for Gibbs phenomena, the amplitude of these oscillations does not decrease with $M$, as can be observed in Fig. 3(b) when $k_{\mathrm{Max}} = 200$; close to the discontinuity point of $f$ and $g$, the continuous function $h_0^{(M,\mathrm{direct})}$ reconstructed by using the direct factorization rule still exhibits oscillatory behavior. On the other hand, with the inverse rule, Fig. 3(c), such oscillations are absent, and even quite low values of $k_{\mathrm{Max}}$ are sufficient for accurate reconstruction of the function $h(r)$.

## 5. CONCLUSION

The factorization rules, developed by Li for functions represented in a truncated exponential basis and applied with great success in the differential theory of gratings,[7] are extended to any truncated basis of continuous functions. Numerical examples show the usefulness of the inverse rule in factorizing the continuous product of discontinuous functions. This study is devoted to the extension of the fast Fourier factorization method[7] to diffraction problems described in non-Cartesian coordinates and, in particular, in cylindrical geometry. Domains of physics other than electromagnetism could also be considered.

E. Popov's e-mail address is e.popov@fresnel.fr.

## REFERENCES

1. L. Li, "Use of Fourier series in the analysis of discontinuous periodic structures," J. Opt. Soc. Am. A **13**, 1870–1876 (1996).
2. J. Jarem, "Rigorous coupled wave analysis of radially and azimuthally-inhomogeneous, elliptical, cylindrical systems," Prog. Electromagn. Res. (PIER) **34**, 89–115 (2001).
3. P. Banerjee and J. Jarem, "Convergence of electromagnetic field components across discontinuous permittivity profiles," J. Opt. Soc. Am. A **17**, 491–492 (2000).
4. P. Lalanne and G. Morris, "Highly improved convergence of the coupled-wave method for TM polarization," J. Opt. Soc. Am. A **13**, 779–784 (1996).
5. G. Granet and B. Guizal, "Efficient implementation of the coupled-wave method for metallic gratings in TM polarization," J. Opt. Soc. Am. A **13**, 1019–1023 (1996).
6. L. Schwartz, *Méthodes Mathématiques pour les Sciences Physiques* (Hermann, Paris, 1961), p. 174.
7. M. Nevière and E. Popov, *Light Propagation in Periodic Media: Differential Theory and Design* (Marcel Dekker, New York, 2003).